Electron transport in folded graphene junctions

Yuee Xie, Yuanping Chen, Xiao Lin Wei, and Jianxin Zhong

Phys. Rev. B **86**, 195426 — Published 26 November 2012

DOI: 10.1103/PhysRevB.86.195426

Electron transport in graphene folding junctions

Yuee Xie, Yuanping Chen,* Xiao Lin Wei, and Jianxin Zhong
Institute for Quantum Engineering and Micro-Nano Energy Technology and Department of Physics, Xiangtan University, Xiangtan 411105, China
(Dated: November 9, 2012)

Using Green's function method, electron transport in graphene folding junctions (GFJs) are studied. All of these junctions are bilayer structures with AA or AB stacking. As for the AA-stacking GFJs, their transport properties are strongly dependent on the edge form and folding angle. The armchair GFJs (AGFJs) with a folding angle of 60^0 have high reflection to electrons, while those with a folding angle of 120^0 are nearly reflectionless and transparent. The zigzag GFJs (ZGFJs) show an opposite transport behavior: the junctions with a folding angle of 60^0 are nearly transparent while those of folding angle 120^0 have high reflection. As for the AB-stacking GFJs, their transport properties are insensitive to the edge form or folding angle, and all junctions exhibit less reflection to electrons. In addition, interesting edge states different from those in the unfolded nanoribbons are found in the GFJs. Our results indicate that GFJs can be served either as resistors for tuning attenuation of currents or as interconnects for changing directions of current in all graphene-based nano-electronics.

PACS numbers: 73.21.-b, 81.05.Uw
Keywords: graphene nanojunction; folding nanostructure; electron transport

I. INTRODUCTION

Graphene is an atomically thin sheet[1,2]. By etching or patterning methods, various nanoribbons[3,4], nanojunctions[5–7] and nanocircuits[8] can be obtained from a single graphene sheet, similar to the paper cutting. So "paper-cutting electronics" has been proposed based on the fact that one can utilize cutting geometry to tune transport properties of graphene[9,10]. Interestingly, graphene not only can be cut like a piece of paper, but also can be folded like paper. Although graphene is stiff in the planar direction[11], it can be easily warped in the out-of-plane direction[12–21]. The orientation or location of folding can be controled[17–20], and the folding bilayer structures are mostly AA or AB stacking. After folding, the electronic properties of graphene or graphene nanoribbons are significantly changed[21–25]. The energy band of folded graphene transits from symmetrical to asymmetrical due to the interlayer interaction and the closed boundary[22]. The energy gaps of folded armchair nanoribbons decrease, and the decrease value depends on the interlayer displacement[23]. Some exotic quantum transport phenomena are also observed in the folded graphene or folded nanoribbons, such as odd and even coexisting conductance steps[23], transition from metal to half-metal[24], and zero energy edge states (a kind of effectively chiral one-dimensional channels)[25], etc. These studies imply that folding is a very effective method to tune electric properties of graphene. So, one can fold graphene (or nanoribbons) into various nanodevice and even all-graphene nanocircuits similar to paper folding. Compared with the single layer graphene-based nanodevices, the nanodevices based on the folded graphene are bilayer structures and thus possess a great advantage: their electronic properties can be tuned continuously and reversibly by adjusting the interlayer atomic displacement. In this novel "paper-folding electronics", graphene junctions folded by nanoribbons are most attractive, because they could be served not only as the basic elements but also as the interconnects for wiring individual circuite elements. However, recent attentions have been only focused on folding nanoribbons into one-dimensional ribbon structures[22–25]. The graphene folding junctions (GFJs) formed by folding nanoribbons along other directions have not been studied so far.

In this paper, we study electron transport in the GFJs which are bilayer structures folded by single-layer nanoribbons. Because the folded graphene found in the experiment are mostly AA or AB stacking[12,13], here we only consider AA- or AB-stacking GFJs, even if maybe they have some other stacking forms[26]. In case of AA or AB stacking, all GFJs only have two folding angles, i.e., 60^0 and 120^0, as shown in Figs. 1(a-f). As for the AA-stacking GFJs in Figs. 1(a-d), it is found that the edge form and folding angle have significant effect on their transport properties. The electron transport in armchair GFJs (AGFJs) is quite different from that in zigzag GFJs (ZGFJs). For example, the AGFJs with a folding angle of 60^0 (60^0-AGFJs) show high reflection as electrons transmit across the junction, while the ZGFJs with the same folding angle are reflectionless to electrons; the AGFJs with a folding angle of 120^0 (120^0-AGFJs) are nearly reflectionless and transparent to electrons, while ZGFJs with the same angle have high reflection. The different transport properties of these junctions are originated from their different inter-layer coupling forms. As for the AB-stacking GFJs in Figs. 1(e-f), electron transport in them is less sensitive to folding angle or edge forms, and all junctions show less reflection to electrons. The transport characteristics of these GFJs become more prominent with the increase of their width or the decrease of their inter-layer distance. Therefore, different type of GFJs can maybe serve as different electrical elements. Some can be used as resistors in the nanocircuits, such as AA-staking 60^0-AGFJ; while some can be used as reflectionless interconnects to change current direction, such as AA-stacking 120^0-AGFJs. In addition, interesting edge states are found in the AA-stacking ZGFJs. The edge states, transmitting toward the folding area from one layer, are forced to change direction and move onto the opposite edge of the other layer after crossing the folding junction.

II. MODEL AND METHOD

The GFJs we considered are shown in Figs. 1(a-f). All of these junctions consist of a central scattering region and two semi-infinite nanoribbons. The central scattering region includes a nanotube-like fold (red atoms) and a finite triangle stacking region (blue atoms). As mentioned above, the stacking form of the finite triangle region is AA or AB stacking. In case of AA stacking, the AGFJs only have two types. One is 60^0-AGFJs, the other is 120^0-AGFJs, as shown in Figs. 1(a) and 1(b), respectively. The AA-stacking ZGFJs also have two types: ZGFJs with a folding angle of 60^0 (60^0-ZGFJs) in Fig. 1(c) and ZGFJs with a folding angle of 120^0 (120^0-ZGFJs) in Fig. 1(d). In case of AB stacking, both AGFJs and ZGFJs only have one type, i.e., 120^0-AGFJ in Fig. 1(e) and 60^0-ZGFJ in Fig. 1(f). The widths of AGFJ and ZGFJ are labeled by N_A (dimer chains) and N_Z (zigzag chains), respectively. In these junctions, the folds (red atoms) are parts of armchair or zigzag nanotubes. For example, in Figs. 1(b), 1(c), 1(e) and 1(f) the folds are parts of armchair nanotubes with a radius about 0.53nm; while in Figs. 1(a) and 1(d) the folds are parts of zigzag nanotubes with a radius about 0.52nm. After the curvature effect (strains in the fold) is omitted, the

nearest-neighbor tight-binding model,

$$H = t \sum_{<i,j>} (c_i^\dagger c_j + H.C.) + V \sum_{<l,m>} (c_l^\dagger c_m + H.c.), \tag{1}$$

can be used to describe the electronic properties of these junctions, where t represents the intra-layer hopping energy, and V is the inter-layer hopping energy only existing in the finite triangle stacking regions (see the blue atoms). The Green's function method can be used to calculate transport properties of these junctions[27]. According to the Green's function scheme, the Green's function of the structure is expressed as

$$G_S = [E - H_0 - \Sigma_L - \Sigma_R]^{-1}, \tag{2}$$

where H_0 is the Hamiltonian of the central scattering region, and $\Sigma_{L,R}$ is the self-energy of the left or right lead. The self-energies can be calculated by the recursive Green's function method[28]. Once the total Green's function G_S is obtained, one can calculate the conductance and the density of state (DOS)

$$G = \frac{2e^2}{h} Tr[\Gamma_L G_S^\dagger \Gamma_R G_S], \tag{3}$$

$$D = -ImTr[G_S]/\pi, \tag{4}$$

where $\Gamma_{L,R} = i[\Sigma_{L,R} - \Sigma_{L,R}^*]$ is the coupling function of the lead[28].

It is noted that the calculations of DFT method demonstrate that the geometries of the GFJs are very complicated[26]. The fold shape, fold radius, inter-layer distance and stacking forms are all associated tightly with the initial structures. Here we focus on the effect of stacking form, folding angle and edge style on the transport properties of GFJs, so the shapes of folds are fixed and the curvature effect of fold is omitted.

III. RESULTS AND DISCUSSION

In Fig. 2, the conductance as a function of electron energy for AA-stacking 60^0- and 120^0-AGFJs are shown. One can find that the folding angle has no effect on the energy gap. Both 60^0-AGFJ and 120^0-AGFJ are metallic as their widths $N_A = 14$, and they have the same energy gap as $N_A = 13$ (see the inset). However, one can find that the folding angle has significant influence on the transport properties. The conductance of 120^0-AGFJ is symmetric around the Fermi energy and conductance steps appear in the profile (see the dashed line), which is similar to the case of unfolded armchair nanoribbon. While the conductance of 60^0-AGFJ is asymmetric and the conductance steps are destroyed by oscillations (see the solid line). Moreover, the conductance of 60^0-AGFJ is lower than that of 120^0-AGFJ. This indicates that electrons can transmit across the junction of angle 120^0 without reflection, but suffer reflection in the junction of angle 60^0.

The difference of transport properties between 60^0-AGFJ and 120^0-AGFJ become more prominent as their width increases. Figure 3(a) shows the conductance of 60^0-AGFJ with three different width N_A. The wider the width of the junction, the lower the conductance of electrons around the Fermi energy, i.e., the higher the reflection in the junction. Therefore, the reflection in the junction increases with the width. This point is more clearly reflected by the inset in Fig. 3(a). The conductance gradually decreases with the increase of width, at last the electron transport is blocked completely by the wider junction. As a comparison, Figure 3(b) shows the conductance of 120^0-AGFJs with different width. One can find that the middle conductance step maintains very well as the width increases. The variation of width just varies the range of the step. Therefore the electron transport in the 120^0-AGFJ is insensitive to the width. Electrons can transmit across the junctions without reflection even in the very wider junctions.

Why transport properties of the two AA-stacking AGFJs have so much difference? It can be explained by different inter-layer coupling form of the two structures. It is known that graphene nanoribbons consist of A and B, two triangle sublattices. The interaction between A and B atoms is called AB coupling, while the interaction between A atoms (or B atoms) is called AA (or BB) coupling. The coupling of intra-layer nearest-neighbor atoms in the unfolded nanoribbons is AB coupling. Seen from Fig. 1(h), the atoms in armchair or zigzag nanoribbons are AA (or BB) symmetric about the solid line. The 60^0-AGFJ can be obtained by folding the armchair nanoribbon along the solid line, therefore, after folding the coupling of inter-layer nearest-neighbor atoms is AA (or BB) coupling. In this case, the inter-layer coupling and the intra-layer coupling in the junction are different. The incompatible coupling form destroys the symmetry of conductance and results in high reflection to electrons. However, the 120^0-AGFJ is obtained by folding the armchair nanoribbon along the dashed line in Fig. 1(h). After folding, the inter-layer and

intra-layer coupling forms in the junction are consistent, namely, both have AB coupling, which leads to reflectionless transmission in the junction. So, although the 60^0-AGFJ in Fig. 1(a) and the 120^0-AGFJ in Fig. 1(b) are both AA stacking, the different inter-layer coupling forms of the two structures result in different transport behaviors.

The inter-layer distance of GFJs can be changed by the stress perpendicular to the layer. The change of distance leads to the variation of the inter-layer hopping energy V. The smaller the distance, the larger the inter-layer hopping energy. We examine the stress effect on the electron transport in the GFJs by changing V. Figures 3(c) and 3(d) show respectively the conductance of AA-stacking 60^0-AGFJs and 120^0-AGFJs with different hopping energy V. One can find that the effect of changing inter-layer hopping energy on conductance is similar to that of changing the nanoribbon width. The conductance of 60^0-AGFJ decreases with the increase of hopping energy V (see fig. 3(c)), indicating that the reflection in the junction can be tuned by the perpendicular stress. While the conductance step of 120^0-AGFJ nearly does not change with the hopping energy (see Fig. 3(d)), indicating that the junction is reflectionless to electrons even under large perpendicular stress.

From the results in Fig. 3, one can conclude that, AA-stacking 60^0-AGFJs can serve as current attenuations analogous to resistors, and stronger attenuation can be obtained by serial combination of junctions; while AA-stacking 120^0-AGFJs can be used as a robust reflectionless interconnect to change current direction.

Figures 4(a) and 4(b) show the conductance profiles for AA-stacking 60^0-ZGFJs and 120^0-ZGFJs, respectively. Firstly, one can see that the conductance profiles of both ZGFJs display a complicated behavior around the Fermi energy, where some sharp conductance peaks appear. This is due to the existence of edge states in the zigzag structures. Secondly, the folding angle has drastic influence on the transport properties. 60^0-ZGFJs and 120^0-ZGFJs exhibit completely different conductance characteristics. As for the 60^0-ZGFJs, the conductance is symmetric about $E = 0$, and there exist perfect conductance steps[see Fig. 4(a)]. Moreover, the shape of the step maintains very well under the variation of width. Electrons in the energy window of steps can transmit across the junction without reflection. As for the 120^0-ZGFJs, however, there are many oscillation on the conductance profiles (see Fig. 4(b)). The wider the junction width, the more the oscillations in the profiles, i.e., electrons in the junctions suffer high reflection. These indicate that the electron transport in the ZGFJs is opposite to the case in the AGFJs, although the AGFJs and ZGFJs are both AA stacking. The reason can be also explained by different inter-layer coupling forms of the two types of GFJs. The 60^0-AGFJ and 120^0-ZGFJ are both formed by folding nanoribbons along the solid line in Fig. 1(h), while the 60^0-ZGFJ and 120^0-AGFJ are both formed by folding nanoribbons along the dashed line. Therefore, after folding, the inter-layer coupling of 60^0-ZGFJ is the same as that of the 120^0-AGFJ, while the inter-layer coupling of 120^0-ZGFJ is the same as that of the 60^0-AGFJ. The opposite inter-layer coupling forms of the two types of GFJs result in the opposite relationship for their transport properties.

To clearly show the transport properties of AA-stacking ZGFJs, in Figs. 5(a) and 5(b) the conductance and DOS for 60^0- and 120^0-ZGFJs around the Fermi energy are illustrated. One can find from Fig. 5(a) that there are three sharp peaks in the conductance of 60^0-ZGFJ (see solid line). One peak is at $E = 0$ and the other two at $E = \pm 0.021$. These peaks correspond to sharp DOS peaks, indicating that these resonant transmissions are induced by the localized states in the junction. There are two peaks appear at $E = 0.001$ and 0.006 in the conductance of 120^0-ZGFJ. The two peaks also correspond to sharp DOS peaks. Asymmetric shape of the two peaks indicates that they are Fano resonance induced by the localized states. Figure 5(c) shows the LDOS of the localized states in the ZGFJs. All of these states are localized at the edges, i.e., edge states. But these edge states are different from those in the unfolded zigzag nanoribbons. In the unfolded nanoribbons, the edge states always propagate along the same edge. While the edge states in Fig. 5(c) are distributed at the opposite edges of two layers, which are somewhat similar to the "zero energy edge states" in Ref.[25]. Electrons propagate firstly along one edge of a giving layer. After crossing the folding area, they are forced to change direction and move onto the opposite edge of the other layer. Meanwhile, the edge states are also correlated with the folding angle of the junctions. For example, at $E = 0$, the edge state in the 60^0-ZGFJ is formed at the outer edges of the junction, while that in the 120^0-ZGFJ is formed at the inner edges of the junction.

Finally, we study electron transport in the AB-stacking GFJs. Figures 6(a) and 6(b) show the conductance of AB-stacking 120^0-AGFJs with different width and inter-layer hopping energy V, respectively. One can find that the transport properties are similar to those of AA-stacking 120^0-AGFJs. The conductance step is insensitive to the width and also insensitive to the inter-layer hopping energy. Therefore, electrons with energies in the step can transmit across this kind of junctions with less reflection. Figure 7 shows the conductance of AB-stacking 60^0-ZGFJs with different width N_Z. Except the energy near $E = 0$, the perfect conductance step maintains very well under the variation of width, indicating that the junctions are reflectionless to the electrons in the energy window of step. This is similar to the case of AA-stacking 60^0-ZGFJs in Fig. 4(a). However, the edge states in the AB-stacking ZGFJs are different from those in the AA-stacking junctions. There exist a perfect edge state on one edge, while the edge state on the other edge disappears due to the inter-layer coupling (see the inset in Fig. 7). Moreover, the edge state only transport along the same edge like that in the unfolded nanoribbons.

IV. CONCLUSIONS

In summary, electron transport in the AA- and AB-stacking GFJs are studied by using the Green's function method. As for the AA-stacking GFJs, their transport properties are strongly dependent on the edge form and folding angle, due to different inter-layer coupling forms. In the 60^0-AGFJ and 120^0-ZGFJ, the inter-layer and intra-layer couplings are different. The incompatible coupling destroys the symmetry of conductance and results in high reflection to electrons. However, in the 120^0-AGFJ and 60^0-ZGFJ, the two coupling forms are consistent and thus these junctions are nearly reflectionless and transparent to electrons. As for the AB-stacking GFJs, the conductance is insensitive to the edge form and folding angle, and all junctions has less reflection to electrons. According to the transport characteristics, the junctions AA-stacking 60^0-AGFJ and 120^0-ZGFJ can serve as resistors in the folded circuits, while the other junctions can act as reflectionless interconnects. In addition, interesting resonant transmissions induced by edge states are found in ZGFJs. Different from the edge states in unfolded zigzag nanoribbons, the edge states in AA-stacking ZGFJs are distributed at different edges of two layers of the junction, which may provide a novel approach to tune spin transport. Finally, we should note that in this paper we omit the influence of the fold, such as the fold shape, fold radius and the curvature effect, on the transport properties of GFJs, which may induce some other interesting transport phenomena. So in the later study we will discuss the effect of these factors.

Acknowledgments

This work was supported by the National Natural Science Foundation of China (Nos. 11074213, 51006086, 51176161, 10774127), the Joint Funds of Hunan Provincial Natural Science Foundation of China (No. 10JJ9001).

* Electronic address: chenyp@xtu.edu.cn

[1] K. S. Novoselov, A. K. Geim, S. V. Morozov, D. Jiang, Y. Zhang, S. V. Dubonos, I. V. Grigorieva, and A. A. Firsov, Science 306 666 (2004).
[2] C. Berger, Z. M. Song, X. B. Li, X. S. Wu, N. Brown, C. Naud, D. Mayou, T. Li, J. Hass, A. N. Marchenkov, et al., Science 312 1191 (2006).
[3] Y. Zhang, Y.-W. Tan, H. L. Stormer, and P. Kim, Nature 438 201 (2005).
[4] B. Biel, X. Blase, F. Triozon, and S. Roche, Phys. Rev. Lett. 102 096803 (2009).
[5] L. C. Campos, V. R. Manfrinato, J. D. Sanchez-Yamagishi, J. Kong, and P. Jarillo-Herrero, Nano Letters 9, 2600 (2009).
[6] X. Wang and H. Dai, Nature Chemistry 2 661 (2010).
[7] A. Iyengar, T. Luo, H. A. Fertig,and L. Brey, Phys. Rev. B 78 235411 (2008).
[8] D. A. Areshkin, D. Gunlycke, and C. T. White, Nano Lett. 7, 204 (2007).
[9] A. K. Geim and K. S. Novoselov, Nature Materials 6 183 (2007).
[10] A. H. Castro Neto, F. Guinea, N. M. R. Peres, K. S. Novoselov,and A. K. Geim, Rev. Mod. Phys. 81 109 (2009).
[11] C. Lee, X. Wei, J. W. Kysar, and J. Hone, Science 321 385 (2008).
[12] Z. Liu, K. Suenaga, P. J. Harris, and S. Iijima, Phys. Rev. Lett. 102 015501 (2009).
[13] J. Zhang, J. Xiao, X. Meng, C. Monroe, Y. Huang, and J. Zuo, Phys. Rev. Lett. 104 166805 (2010).
[14] H. Schmidt, T. Lüdtke, P. Barthold, E. McCann, V. I. Falko, and R. J. Haug, Appl. Phys. Lett. 93 172108 (2008).
[15] X. Li, X. Wang, L. Zhang, S. Lee, and H. Dai, Science 319 1229 (2008).
[16] J. Y. Huang, F. Ding, B. I. Yakobson, P. Lu, L. Qi, and J. Li, PNAS 106 10103 (2009).
[17] A. W. Robertson, A. Bachmatiuk, Y. A. Wu, F. Schäffel, B. Büchner, M. H. Rümmeli, and J. H. Warner, ACS Nano 5 9984 (2011).
[18] S. Eugene, Nature Materials 10 84 (2011).
[19] K. Kim, Z. Lee, B. Malone, K. T. Chan, W. Regan, et al., Phys. Rev. B 83 245433 (2011).
[20] H. C. Schniepp, K. N. Kudin, J. L. Li, R. K. Prud'homme, R. Car, D. A. Saville, and I. A. Aksay, ACS Nano 2 2577 (2008).
[21] Ji Feng, Liang Qi, Jian Yu Huang, and Ju Li, Phys. Rev. B 80 165407 (2009).
[22] Y. Takagi and S. Okada, J. Phys. Soc. Jpn. 79 033702 (2010).
[23] Y. E. Xie, Y. P. Chen,and J. X. Zhong, J. Appl. Phys. 106 103714 (2009).
[24] X. H. Zheng, L. L. Song, R. N. Wang, H. Hao, L. J. Guo, and Z. Zeng, Appl. Phys. Lett. 97 153129 (2010).
[25] E. Prada, P. San-Jose,and L. Brey, Phys. Rev. Lett. 105 106802 (2010).
[26] W. J. Yin, Y. E. Xie, L. M. Liu, Y. P. Chen, R. Z. Wang, and H. M. Lau, *Atomic structure of folded graphene nanoribbons: a first-principles study* (In prepare).
[27] S. Datta, *Electronic Transport in Mesoscopic systems* (Cambridge University Press, Cambridge, U.K., 1997).
[28] Y. P. Chen, Y. E. Xie, and X. H. Yan, J. Appl. Phys. 103 063711 (2008).

Figure Caption

Fig. 1. (Color online) Top view of (a) AA-stacking 60^0-AGFJ; (b) AA-stacking 120^0-AGFJ; (c) AA-stacking 60^0-ZGFJ; (d) AA-stacking 120^0-ZGFJ; (e) AB-stacking 120^0-AGFJ; (f) AB-stacking 60^0-ZGFJ. N_A and N_Z represent the width of AGFJ and ZGFJ, respectively. The blue atoms label overlapping areas of two layers, while the red atoms label the fold. (g) Side view of GFJs which consist of a nanotube-like fold (red atoms) and two semi-infinite nanoribbons. (h) Part of a graphene nanoribbon, which is an armchair nanoribbon if extending along horizontal direction or a zigzag nanoribbon if extending along perpendicular direction. The AA-stacking AGFJs/ZGFJs in (a-d) can be formed by folding the armchair/zigzag nanoribbons along the solid or dashed line.

Fig. 2. (Color online) The conductance as a function of electron energy for the AA-stacking 60^0-AGFJ (solid line) and 120^0-AGFJ (dashed line) with width $N_A = 14$ ($V = 0.1$). Inset: The conductance for the two junctions with width $N_A = 13$.

Fig. 3. The conductance as a function of electron energy for the AA-stacking (a) 60^0-AGFJ and (b) 120^0-AGFJ with different N_A ($V = 0.1$); Inset in (a): The conductance for AA-stacking 60^0-AGFJs as a function of width N_A at $E = 0$ (solid line) and 0.1 (dotted line). The conductance as a function of electron energy for the AA-stacking (c) 60^0-AGFJ and (d) 120^0-AGFJ with different inter-layer hopping energy V ($N_A = 14$).

Fig. 4. (Color online) The conductance as a function of electron energy for the AA-stacking (a) 60^0-ZGFJs and (b) 120^0-ZGFJs with different width N_Z ($V = 0.1$). Solid, dashed and dotted lines represent $N_Z = 8$, 12 and 15, respectively.

Fig. 5. (Color online) The conductance (a) and DOS (b) as a function of electron energy near $E = 0$ for the AA-stacking 60^0-ZGFJ (solid line) and 120^0-ZGFJ (dashed line) ($N_Z = 8$ and $V = 0.1$). (c) The LDOS of localized states in the junctions. Top two are localized states in AA-stacking 60^0-ZGFJ corresponding to DOS peaks at $E = 0$ and $E = \pm 0.021$; Bottom two are localized states in AA-stacking 120^0-ZGFJ corresponding to DOS peaks at $E = 0$ and $E = 0.005$.

Fig. 6. (Color online) (a) The conductance as a function of electron energy for the AB-stacking 120^0-AGFJs with different N_A ($V = 0.1$); (b) The conductance as a function of electron energy for the AB-stacking 120^0-AGFJs with different inter-layer hopping energy V ($N_A = 14$).

Fig. 7. (Color online) The conductance as a function of electron energy for the AB-stacking 60^0-ZGFJs with different width N_Z ($V = 0.1$). Solid, dashed and dotted lines represent $N_Z = 8$, 12 and 15, respectively. Inset: The LDOS of localized states in the junction with $N_Z = 8$ at $E = 0$.

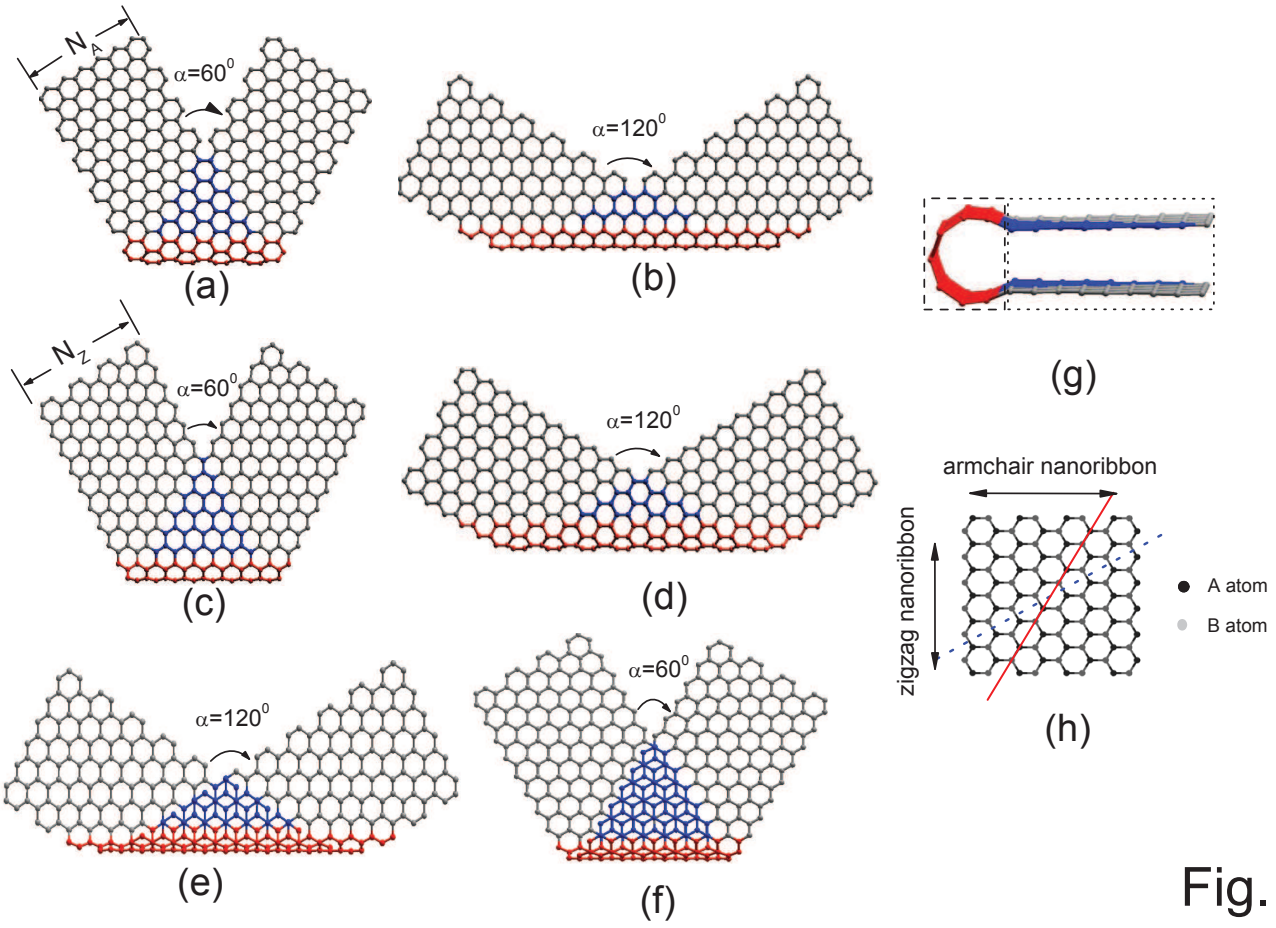

Fig.1

Figure 1 LE13286B 09Nov2012

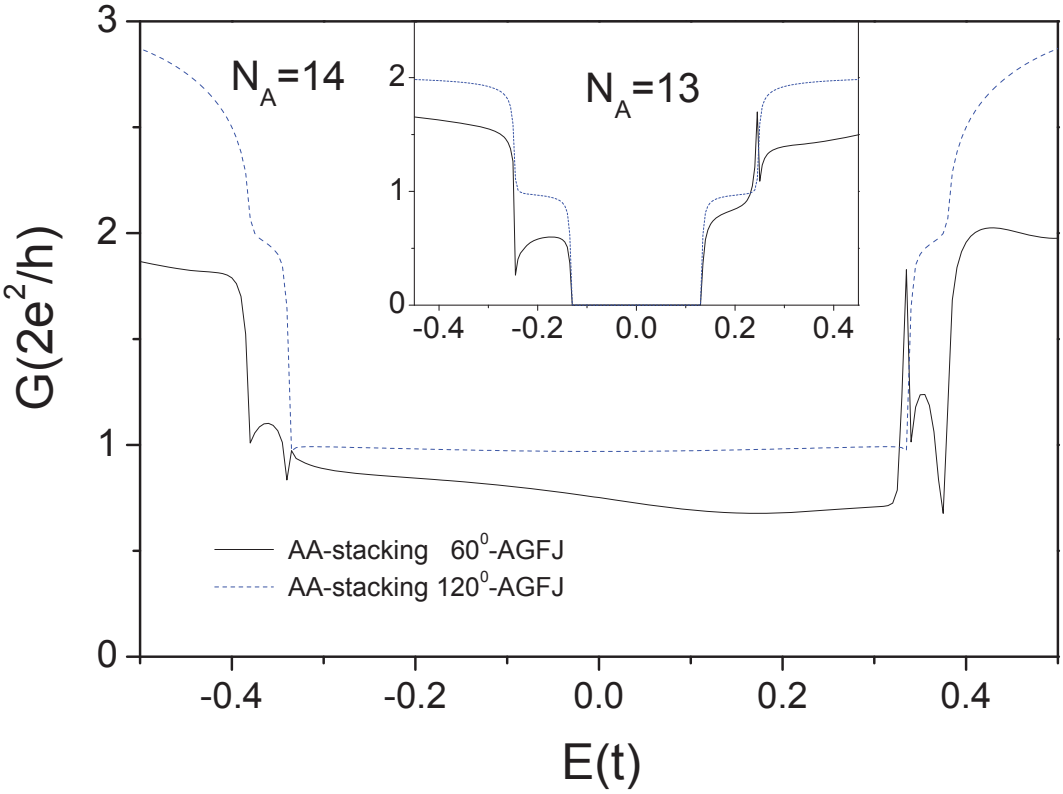

Fig.2

Figure 2 LE13286B 09Nov2012

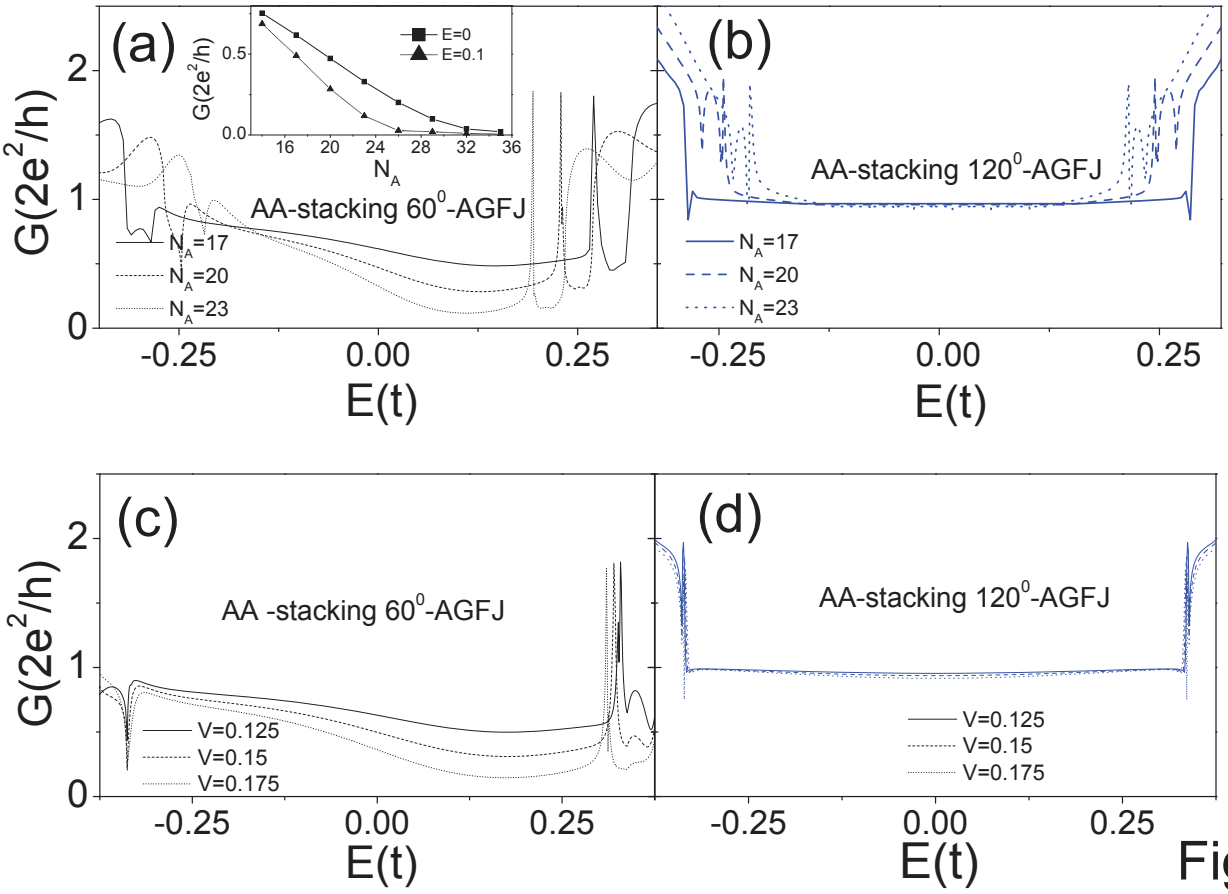

Fig.3

Figure 3 LE13286B 09Nov2012

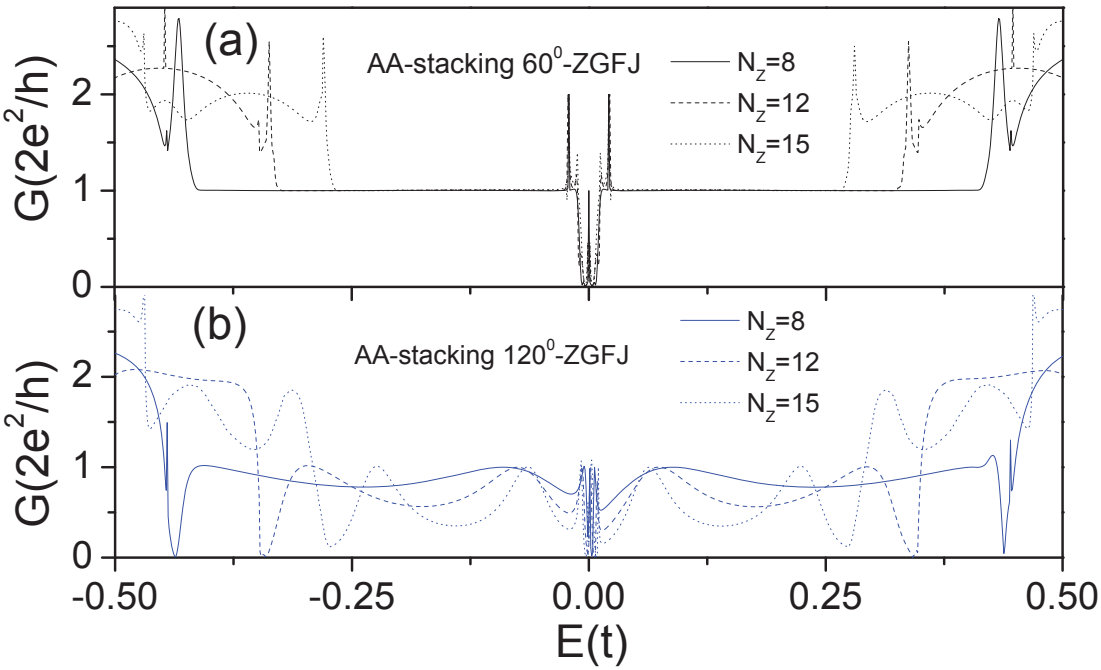

Fig.4

Figure 4 LE13286B 09Nov2012

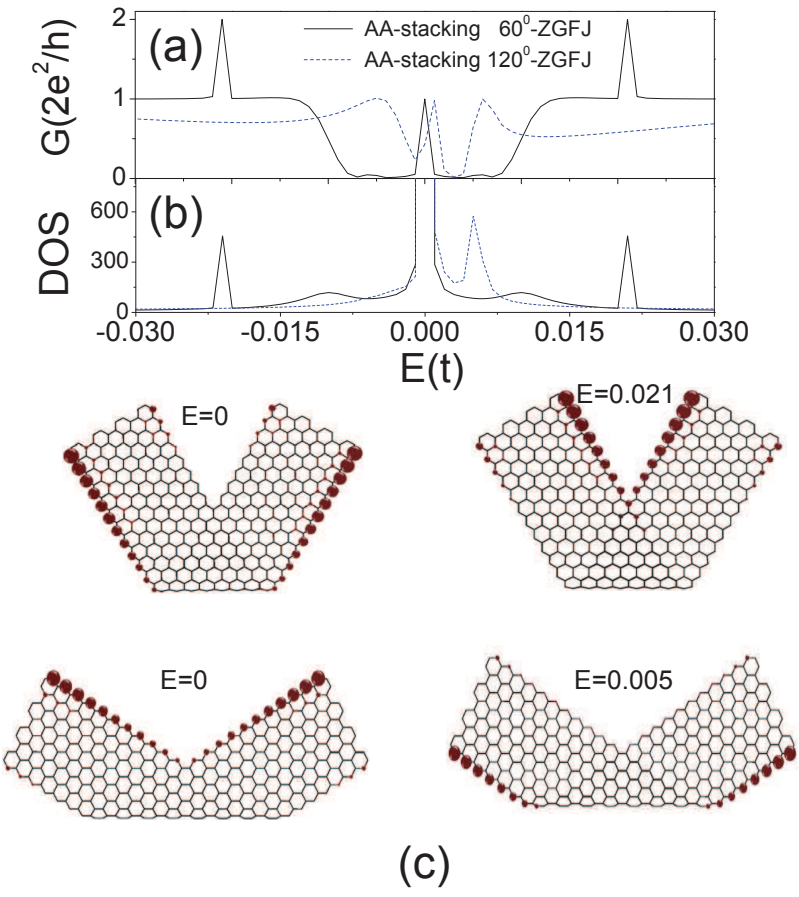

Fig.5

Figure 5 LE13286B 09Nov2012

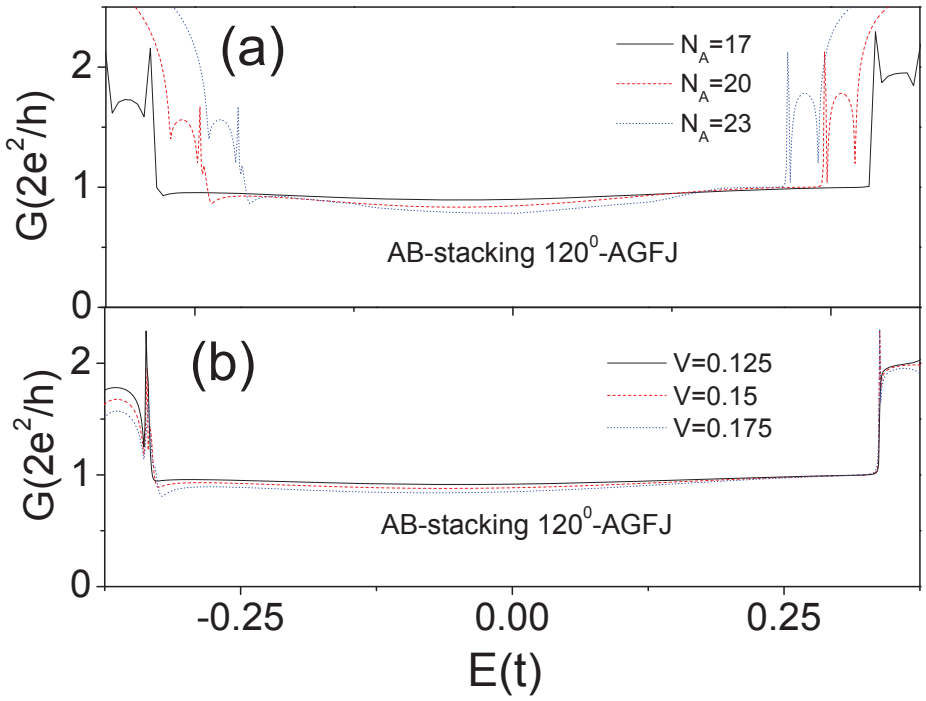

Fig.6

Figure 6 LE13286B 09Nov2012

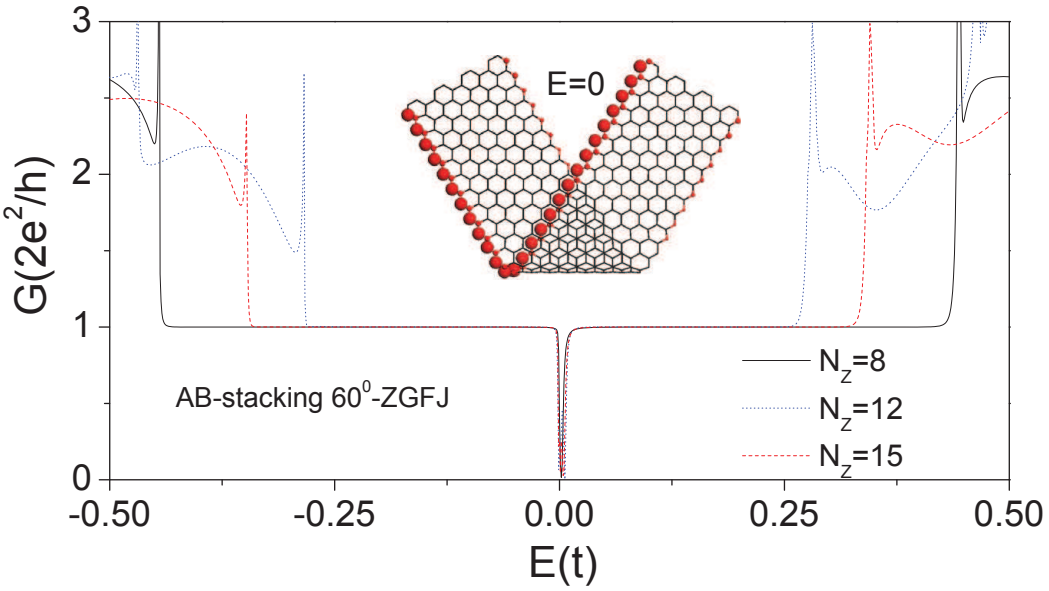

Fig.7

Figure 7 LE13286B 09Nov2012